

## Structural, thermodynamic, and electrical properties of polar fluids and ionic solutions on a hypersphere: Results of simulations

J. M. Caillol and D. Levesque

Citation: [The Journal of Chemical Physics](#) **96**, 1477 (1992); doi: 10.1063/1.462181

View online: <http://dx.doi.org/10.1063/1.462181>

View Table of Contents: <http://scitation.aip.org/content/aip/journal/jcp/96/2?ver=pdfcov>

Published by the [AIP Publishing](#)

---

### Articles you may be interested in

[A new dipolar potential for numerical simulations of polar fluids on the 4D hypersphere](#)

J. Chem. Phys. **141**, 124111 (2014); 10.1063/1.4896181

[Thermodynamical and structural properties of imidazolium based ionic liquids from molecular simulation](#)

J. Chem. Phys. **128**, 154509 (2008); 10.1063/1.2907332

[Monte Carlo simulation and reference hypernetted chain equation results for structural, thermodynamic, and dielectric properties of polar heteronuclear diatomic fluids](#)

J. Chem. Phys. **104**, 6710 (1996); 10.1063/1.471388

[Structural, thermodynamic, and electrical properties of polar fluids and ionic solutions on a hypersphere: Theoretical aspects](#)

J. Chem. Phys. **96**, 1455 (1992); 10.1063/1.462849

[Electrical properties of polarizable ionic solutions. II. Computer simulation results](#)

J. Chem. Phys. **91**, 5555 (1989); 10.1063/1.457558

---

The cover of the AIP Applied Physics Reviews journal. It features a blue and orange color scheme. On the left, there is a small image of the journal cover showing a grid of data. The main text 'NEW Special Topic Sections' is in large, white, sans-serif font. Below it, 'NOW ONLINE' is in yellow, followed by 'Lithium Niobate Properties and Applications: Reviews of Emerging Trends' in white. The AIP Applied Physics Reviews logo is in the bottom right corner.

## NEW Special Topic Sections

**NOW ONLINE**  
Lithium Niobate Properties and Applications:  
Reviews of Emerging Trends

**AIP** Applied Physics  
Reviews

# Structural, thermodynamic, and electrical properties of polar fluids and ionic solutions on a hypersphere: Results of simulations

J. M. Caillol and D. Levesque

Laboratoire de Physique Théorique et Hautes Énergies,<sup>a)</sup> Université Paris-Sud, Bâtiment 211, 91405 Orsay Cédex, France

(Received 28 May 1991; accepted 8 October 1991)

The reliability and the efficiency of a new method suitable for the simulations of dielectric fluids and ionic solutions is established by numerical computations. The efficiency depends on the use of a simulation cell which is the surface of a four-dimensional sphere. The reliability originates from a charge-charge potential solution of the Poisson equation in this confining volume. The computation time, for systems of a few hundred molecules, is reduced by a factor of 2 or 3 compared to this of a simulation performed in a cubic volume with periodic boundary conditions and the Ewald charge-charge potential.

## INTRODUCTION

It has been established in Ref. 1 that a successful method for the simulation of a Coulomb system consists in confining the charged molecules in a three-dimensional (3D) no-Euclidean volume ( $S_3$ ) which is the surface of a 4D sphere, with the condition that the potential between the charges is the solution of the Poisson equation in the  $S_3$  geometry. The main advantage of this isotropic simulation cell compared to the usual cubic volume ( $C_3$ ) with periodic boundary conditions is to allow easily the simulation of inhomogeneous systems in contact with an electrified interface.

In Ref. 1, it was shown that the simulations of a mixture of charged hard spheres (HS) in the  $S_3$  and  $C_3$  geometries give identical results, when, in  $C_3$ , the charge-charge interaction is also the convenient solution of the Poisson equation, i.e., the well-known Ewald potential.<sup>2,3</sup> Furthermore, accurate estimates of the density profiles of this charged HS mixture near an electrified hard wall were obtained in Ref. 1. These computations would have been very difficult to realize by using the Ewald potential adapted to this inhomogeneous system.

These successes of the  $S_3$  simulation method have motivated the present attempt of its application to dielectric fluids and ionic solutions. This extension needs the development of the electrostatic laws in the  $S_3$  closed space and also the expression in this space of the expansion of the two-body correlation functions on a set of rotational invariant functions. Such an expansion is essential for the analysis of the

physically relevant intermolecular correlations. This theoretical work will be published elsewhere.<sup>4</sup> Here, we discuss the numerical simulations which demonstrate the possibility of obtaining reliable estimates of the properties of dielectric fluids and ionic solutions by using the  $S_3$  simulation cell.

In Sec. I, the expression of the ion-ion, ion-dipole, and dipole-dipole interactions and the rotational invariant functions, which are useful for the discussion of the simulation data, are summarized. Section II is devoted to the simulations of homogeneous dielectric fluids, and Sec. III to those of ionic solutions and ionic fluids. For these last systems, our new data complete the results of Ref. 1, because they concern ionic fluids where the charge-charge interaction is modified in order to deal with ionic systems similar to these formed in the  $C_3$  geometry by the replicas of the periodic cells surrounded by a continuous dielectric medium. For the three systems, we examine the size effects. In the conclusion we give the practical rules which should allow performance of Monte Carlo (MC) simulation in  $S_3$  space at the same level of accuracy and reliability as in the usual  $C_3$  geometry.

## I. THEORETICAL SUMMARY

In the  $S_3$  closed space, the potential energy of an ionic solution, composed by  $N_+$  and  $N_-$  HS with charges  $q$  and  $-q$  in a solvent of  $N_d$  dipolar HS is given by the following expression<sup>4</sup> (whether the three species of HS have an identical diameter  $\sigma$ ):

$$\begin{aligned}
 U(\lambda) = & \sum_{i < j = 1}^N v^{\text{HS}}(\psi_{ij}) + \frac{1}{2} \sum_{i \neq j = 1}^{N_i} \Phi_{qq}(\psi_{ij}) + N_i \epsilon_q(\lambda) \\
 & + \sum_{i=1}^{N_i} \sum_{l=1}^{N_d} \Phi_{qd}(\psi_{il}) + \frac{1}{2} \sum_{l \neq m = 1}^{N_d} \Phi_{dd}(\psi_{lm}) + \frac{1}{2} \sum_{i \neq j = 1}^{N_i} \frac{8}{3\pi R} \lambda(\lambda - 2) q_i q_j \cos(\psi_{ij}) \\
 & + \sum_{i=1}^{N_i} \sum_{l=1}^{N_d} \frac{8q_i}{3\pi R^2} \lambda(\lambda - 2) \hat{\mathbf{z}}_i \cdot \boldsymbol{\mu}_l + \frac{1}{2} \sum_{l \neq m = 1}^{N_d} \frac{8}{3\pi R^3} \lambda(\lambda - 2) \boldsymbol{\mu}_l \cdot \boldsymbol{\mu}_m + N_d \epsilon_d(\lambda),
 \end{aligned} \tag{1}$$

<sup>a)</sup> Laboratoire associé au CNRS.

where  $N_+ = N_-$ ,  $N_i = N_+ + N_-$ , and  $N = N_i + N_d$ . By an obvious rearrangement of the terms, the formula (1) can be written as

$$U(\lambda) = U_{ii}(\lambda) + U_{id}(\lambda) + U_{dd}(\lambda),$$

where  $U_{ii}(\lambda)$ ,  $U_{id}(\lambda)$ , and  $U_{dd}(\lambda)$  are, respectively, the ion-ion, ion-dipole, and dipole-dipole partial potential energies. In Eq. (1),  $v^{\text{HS}}(\psi_{ij})$  is the hard-core potential in  $S_3$  space defined by

$$v^{\text{HS}}(\psi_{ij}) = \begin{cases} \infty & \text{if } \sigma/R > \psi_{ij} > 0, \\ 0 & \text{otherwise,} \end{cases} \quad (2)$$

where  $R$  is the radius of the 4D sphere.  $\psi_{ij}$  is the angle between the 4D unit vectors  $\hat{\mathbf{z}}_i$  and  $\hat{\mathbf{z}}_j$  such that  $R\hat{\mathbf{z}}_i$  and  $R\hat{\mathbf{z}}_j$  are the vector positions of the HS  $i$  and  $j$  on the surface of the 4D sphere. The charge  $q_i$  is equal to  $+q$  for  $1 \leq i \leq N_+$  and  $-q$  for  $N_+ + 1 \leq i \leq N_i$ .  $\boldsymbol{\mu}_l (= \mu \hat{\mathbf{s}}_l)$ , a 4D vector of length  $\mu$ , is the dipole moment of the dipolar HS  $l$ , which stays tangent to the 4D sphere. The charge-charge potential  $\Phi_{q,q_j}(\psi_{ij})$  is equal to

$$\Phi_{q,q_j}(\psi_{ij}) = \frac{q_i q_j}{\pi R} \left[ (\pi - \psi_{ij}) \cot \psi_{ij} - \frac{1}{2} \right]. \quad (3)$$

$\Phi_{q,d}(\psi_{ij})$  and  $\Phi_{dd}(\psi_{lm})$ , the charge-dipole and dipole-dipole interactions, can be derived from  $\Phi_{q,q_j}(\psi_{ij})$ , and they have the following expressions:

$$\Phi_{q,d}(\psi_{il}) = \frac{q_i}{\pi R^2} \left( \cot \psi_{il} + \frac{\pi - \psi_{il}}{\sin^2 \psi_{il}} \right) \frac{\hat{\mathbf{z}}_i \cdot \boldsymbol{\mu}_l}{\sin \psi_{il}}, \quad (4)$$

and

$$\begin{aligned} \Phi_{dd}(\psi_{lm}) = & \frac{1}{\pi R^3} \left\{ \frac{2}{\sin^2 \psi_{lm}} (\hat{\mathbf{z}}_m \cdot \boldsymbol{\mu}_l) (\hat{\mathbf{z}}_l \cdot \boldsymbol{\mu}_m) \right. \\ & + \frac{1}{\sin \psi_{lm}} \left( \cot \psi_{lm} + \frac{\pi - \psi_{lm}}{\sin^2 \psi_{lm}} \right) \\ & \times \left[ \boldsymbol{\mu}_l \cdot \boldsymbol{\mu}_m + 3 \cot \psi_{lm} \frac{(\hat{\mathbf{z}}_m \cdot \boldsymbol{\mu}_l) (\hat{\mathbf{z}}_l \cdot \boldsymbol{\mu}_m)}{\sin \psi_{lm}} \right] \left. \right\}. \end{aligned} \quad (5)$$

In the Eq. (1), the terms depending on the parameter  $\lambda$  allow us to include in the  $S_3$  geometry, physical constraints identical to these induced in the  $C_3$  geometry by a dielectric continuum of dielectric constant  $\epsilon'$  surrounding the replicas of the simulation cell. These terms can be summarized in a unique term which includes the contribution of the charge and dipole self-energies  $\epsilon_q(\lambda)$  and  $\epsilon_d(\lambda)$  depending on  $\lambda$ :

$$2\lambda(\lambda - 2) \frac{4\pi}{3V} (\mathbf{M}_i + \mathbf{M}_d)^2 \equiv 2\lambda(\lambda - 2) \frac{4\pi}{3V} \mathbf{M}^2$$

with  $\mathbf{M}_i = R \sum_j q_j \hat{\mathbf{z}}_j$ ,  $\mathbf{M}_d = \sum_l \boldsymbol{\mu}_l$ , and  $V = 2\pi^2 R^3$  (volume of the 4D sphere). The expressions of these self-energies are

$$\begin{aligned} \epsilon_q(\lambda) = & \frac{q^2}{2\pi R} \left[ \frac{1}{2} + (\pi - 2\delta) \cot \delta - \frac{\pi}{\sin \delta} \right] \\ & + \frac{4q^2}{3\pi R} \lambda(\lambda - 2) \end{aligned} \quad (6)$$

with  $\delta = \sigma/2R$  and

$$\epsilon_d(\lambda) = \frac{4\mu^2}{3\pi R^3} \lambda(\lambda - 2). \quad (7)$$

The justification of the expression of  $U(\lambda)$  is made in Ref. 4; it needs a careful extension of the derivation schemes of the electrostatic energy used in the 3D Euclidean space or in the  $C_3$  geometry.<sup>2,3</sup> In Ref. 4, the similarity between  $U(\lambda)$  and the Ewald energy of an ionic solution is demonstrated whether the following relation connects  $\lambda$  and  $\epsilon'$ :

$$(\lambda - 1)^2 = \frac{1}{2\epsilon' + 1}. \quad (8)$$

In the  $S_3$  geometry, it is possible to derive the Stillinger-Lovett (SL) rule which expresses the screening of a charge by the other ions and the solvent molecules; the general form of the SL rule in  $S_3$  is

$$\frac{4\pi\beta}{3V} \langle \mathbf{M}^2 \rangle = \frac{1}{(\lambda - 1)^2} \quad (9a)$$

and

$$\frac{4\pi\beta}{3V} (\langle \mathbf{M}_d^2 \rangle + \langle \mathbf{M}_i \cdot \mathbf{M}_d \rangle) = 0, \quad (9b)$$

where  $\langle \dots \rangle$  denotes an ensemble average and  $\beta = 1/kT$ .

The dielectric constant  $\epsilon$  of homogeneous dielectric fluids is given by

$$\frac{4\pi\beta}{3V} \langle \mathbf{M}_d^2 \rangle = \frac{\epsilon - 1}{1 + (\lambda - 1)^2(\epsilon - 1)} = \frac{(\epsilon - 1)(2\epsilon' + 1)}{2\epsilon' + \epsilon}. \quad (10)$$

The last equation is obtained from relation (8). It is identical to the relation between  $\langle \mathbf{M}_d^2 \rangle$ ,  $\epsilon$ , and  $\epsilon'$  in the  $C_3$  geometry. In the 3D Euclidean space, the analysis of the molecular correlations in the ionic solutions is made by expanding the two-body correlation functions on a complete set of rotational invariant functions. The most important terms of this expansion are denoted  $g_{ii}^{000}(r)$ ,  $g_{id}^{000}(r)$ ,  $g_{dd}^{000}(r)$ ,  $g_{id}^{011}(r)$ ,  $g_{di}^{101}(r)$ ,  $g_{dd}^{110}(r)$ , and  $g_{dd}^{112}(r)$ , where the indices  $i$  or  $d$  denote, respectively, an ion or a solvent molecule. The three functions of type  $g^{000}(r)$  characterize the structural arrangement of the ions and the solvent; the functions  $g_{id}^{011}(r)$ ,  $g_{di}^{101}(r)$ , and  $g_{dd}^{112}(r)$  give the average orientation of the dipoles in the electric field of an ion or a solvent molecule.  $g_{dd}^{110}(r)$  is the average orientation of two dipoles separated by a distance  $r$ .

In  $S_3$ , the functions  $g^{lmn}$  depend on  $R\psi_{ij}$ , the length of the geodesic between two molecules  $l$  and  $j$ . These functions are computed from the following ensemble averages where the indices  $a$  and  $b$  may be equal to  $i$  or  $d$ :

$$\begin{aligned} g_{ab}^{lmn}(\psi) = & c_{ab}^{lmn} \frac{1}{N_a \rho_b} \left\langle \sum_{k=1}^{N_a} \sum_{j=1}^{N_b} * \chi(k,j) \Phi^{lmn}(k,j) \right\rangle \\ & \times \frac{1}{4\pi R^3 \sin \psi \delta \psi}. \end{aligned} \quad (11)$$

$\Sigma^*$  indicates that the term  $j = k$  is omitted for  $a = b$ ,  $\rho_b = N_b/V$ , and  $c_{ab}^{000} = 1$ ,  $c_{id}^{011} = 6$ ,  $c_{dd}^{110} = 3$ , and  $c_{dd}^{112} = 3/2$ .  $\chi(k,j)$  and  $\Phi^{lmn}(k,j)$  are defined by

$$\chi(k,j) = \begin{cases} 1 & \text{if } \psi < \psi_{kj} < \psi + \delta\psi, \\ 0 & \text{otherwise.} \end{cases}$$

$$\Phi^{000}(k,j) = 1,$$

$$\Phi^{101}(k,j) = -\Phi^{011}(k,j) = \frac{\hat{\mathbf{s}}_k \cdot \hat{\mathbf{z}}_j}{\sin \psi_{kj}},$$

$$\Phi^{110}(k,j) = \hat{s}_k \cdot \hat{s}_j - \frac{1}{1 + \cos \psi_{kj}} (\hat{s}_k \cdot \hat{z}_j) (\hat{s}_j \cdot \hat{z}_k),$$

$$\Phi^{112}(k,j) = -\hat{s}_k \cdot \hat{s}_j - \frac{2 + \cos \psi_{kj}}{\sin^2 \psi_{kj}} (\hat{s}_k \cdot \hat{z}_j) (\hat{s}_j \cdot \hat{z}_k). \quad (12)$$

These expressions of  $\Phi^{lmn}(k,j)$  are justified in Ref. 4; the  $\Phi^{lmn}(k,j)$  functions are invariant under the simultaneous rotation of the molecules  $k$  and  $j$  in the  $S_3$  space and are orthogonal with respect to the convenient scalar product in this space. By using Eq. (11), the pressure  $P$  is given by the formula (cf. Ref. 5 where the expression of  $P$  has been derived for the HS system in  $S_3$ )

$$\frac{\beta P}{\rho} = 1 + \frac{4\pi}{3} R^2 \rho \sin^2 \psi_0 [x_+^2 g_{++}^{000}(\sigma) + x_-^2 g_{--}^{000}(\sigma)]$$

$$+ \frac{1}{3} \beta U_{ii}(\lambda) + \frac{8\pi}{3} R^2 \rho \sin^2 \psi_0 x_+ x_a g_{ia}^{000}(\sigma)$$

$$+ \frac{1}{3} \beta U_{ia}(\lambda) + \frac{4\pi}{3} R^2 \rho \sin^2 \psi_0 x_a^2 g_{aa}^{000}(\sigma)$$

$$+ \frac{1}{3} \beta U_{dd}(\lambda), \quad (13)$$

where  $\rho = N\sigma^3/V$ ,  $x_+ = N_+/N$ ,  $x_- = N_-/N$ ,  $x_a = N_a/N$ , and  $\psi_0 = \sigma/R$ .

The potential energy  $U(\lambda)$ , the definitions (11) and (12), the formulas (10) and (13), and the expressions (9) of the SL rule allow us to realize a significant comparison of the  $C_3$  and  $S_3$  simulations.

## II. SIMULATIONS OF HOMOGENEOUS DIELECTRIC FLUIDS

The simulations of the homogeneous dielectric fluids were performed in order to estimate the values of  $N$ , where the results obtained for the  $C_3$  and  $S_3$  geometries become identical, and to establish the possibility of computing in  $S_3$  the dielectric constant. The potential energy of the considered system of polar HS is easily deduced from expression (1) of  $U(\lambda)$  in setting to zero the ion-ion and ion-dipole partial energies.

The extensive computations of dipolar soft-sphere systems realized by Kusalik<sup>6</sup> in the  $C_3$  geometry give an unambiguous estimate of the size dependencies of the simulation data. From the results of Ref. 6 for the systems of size:  $N = 108, 256, 500$ , and  $1372$ , it can be asserted that their thermodynamic properties do not differ by more than  $\sim 0.5\%$  in this range of  $N$  values and that, for  $N > 256$ , there is no systematic trend to an increase or decrease on these quantities characteristic of size effects. Then, the value of  $N = 256$  seems sufficient for a reliable calculation of the internal energy and the pressure in  $C_3$  geometry. For the estimate of  $\epsilon$  a similar conclusion can be made. For instance, for  $\epsilon' = \infty$  all the computed values of  $\epsilon$  are compatible within the statistical uncertainties for  $N > 256$ . Considering the similarity of the polar hard- and soft-sphere systems, we estimate that, in Table I, the simulation data, in  $C_3$ , for  $N = 256$ ,  $\epsilon' = \infty$  or  $\epsilon' = 0$ , and  $\rho = 0.8$  at  $\mu^{*2} (= \mu^2/kT\sigma^3) = 2.0$  or  $2.75$  give the values of the internal energy and the pressure

TABLE I. Simulations data of homogeneous dielectric fluid at  $\rho = 0.8$ . The symbols have been defined in the text (cf. Sec. I).  $U_{dd} = \langle U_{dd}(\lambda) \rangle$ ,  $n$  is the number of trial moves per particle. For the  $C_3$  simulations, the two quoted values of  $\epsilon$  are computed by using  $\langle M_d^2 \rangle$  and  $\langle M_d^2 \rangle - \langle M_d \rangle^2$ , two estimates of the dipole moment fluctuations. The statistical uncertainties correspond to the error on the last digit of the average values.

$\mu^{*2}$	$N$	$n \times 10^4$	$U_{dd}$	$\bar{M}_{d,\alpha}$	$\epsilon$	$g_{dd}^{000}(\sigma)$	$g_{dd}^{112}(\sigma)$	$g_{dd}^{110}(\sigma)$	$\lambda/\epsilon'$
2	864	11	-2.757 ± (2)	0.01 ± (1)	35 ± (4)	4.718 ± (4)	4.539 ± (8)	3.49 ± (3)	1.0
	512	10	-2.770 ± (2)	0.02 ± (2)	40 ± (5)	4.734 ± (2)	4.57 ± (1)	3.56 ± (2)	1.0
	256	10	-2.811 ± (5)	0.08 ± (3)	64 ± (10)	4.71 ± (1)	4.45 ± (2)	3.97 ± (7)	1.0
	256	20	-2.773 ± (2)	0.01 ± (1)	66 ± (7)	4.740 ± (5)	4.60 ± (1)	3.60 ± (2)	0.8
	256	8	-2.764 ± (4)	0.001 ± (1)	...	4.732 ± (5)	4.63 ± (1)	3.49 ± (6)	0
	256	10	-2.730 ± (3)	0.04 ± (2)	33 ± (5)	4.77 ± (1)	4.51 ± (2)	3.47 ± (4)	$\infty$
	256	20	-2.722 ± (2)	0.01 ± (2)	29 ± (3)	4.749 ± (7)	4.49 ± (1)	3.41 ± (2)	31
	256	4.0	-4.184	0.002 ± (2)	...	5.20 ± (2)	5.72 ± (2)	4.89 ± (3)	0
2.75	256	8.5	-4.21 ± (1)	0.003 ± (3)	...	5.26 ± (1)	5.96 ± (2)	4.7 ± (2)	0
	256	20	-4.200 ± (2)	0.05 ± (3)	63 ± (6)	5.23 ± (1)	5.70 ± (2)	5.11 ± (4)	$\infty$
	256	20	-4.200 ± (2)	0.05 ± (3)	59 ± (6)	5.23 ± (1)	5.70 ± (2)	5.11 ± (4)	$\infty$

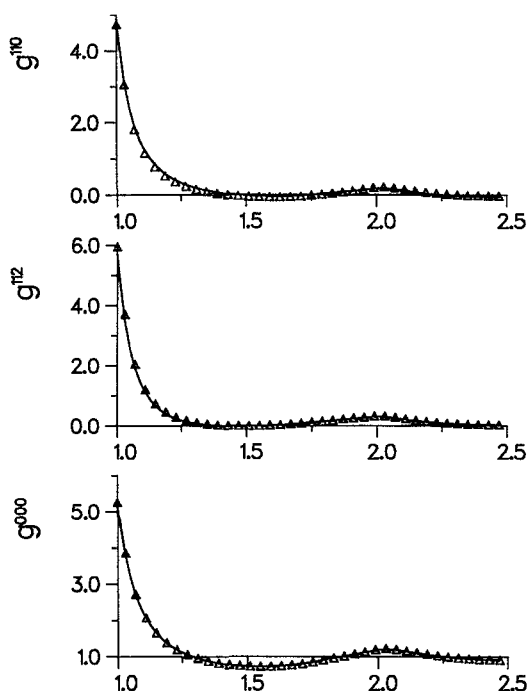


FIG. 1. From bottom to top, comparison between the  $g^{lmn}$  functions of homogeneous dielectric fluids computed for  $\mu^{*2} = 2.75$ ,  $N = 256$ , and  $\rho = 0.8$  in the  $C_3$  geometry (continuous line) at  $\epsilon' = 0$  and the  $S_3$  geometry (open triangles) at  $\lambda = 0$ .  $r$  is equal to the 3D distance in  $C_3$  and to  $R\psi$  in  $S_3$ .

which should be obtained by a reliable simulation in the  $S_3$  geometry.

This agreement is found within a discrepancy of  $\sim 2\%$  for the results of  $S_3$  simulations performed with  $\lambda = 0$  and  $N = 256$  both for the thermodynamic properties and the correlation functions (cf. Fig. 1). The calculation of  $\epsilon$  has been made in  $C_3$  geometry for  $\epsilon' = \infty$  and  $\epsilon' = 31$  at  $\mu^{*2} = 2$  and for  $\epsilon' = \infty$  at  $\mu^{*2} = 2.75$ . The estimated values are  $\epsilon \sim 33 \pm 5$  ( $\mu^{*2} = 2$ ) and  $\epsilon \sim 60 \pm 6$  ( $\mu^{*2} = 2.75$ ). In  $S_3$ , the value  $\lambda = 0$  corresponds to  $\epsilon' = 0$ , which precludes the computation of  $\epsilon$  because the relation (10) has the form  $(\epsilon - 1)/\epsilon = 4\pi\beta \langle \mathbf{M}_d^2 \rangle / 3V$ .

When the simulations are realized for  $\lambda \neq 0$ , there are strong size effects and the results of  $C_3$  geometry are recovered only for systems with  $N \sim 864$ . This size dependence is due to the polarization of the system under the influence of the interaction terms depending on  $\lambda$ . In Table I, the quantity  $\bar{M}_{d,\alpha}$ , which is the maximum of the average values of the four components of  $\mathbf{M}_d/N$ , shows clearly this effect. For  $\lambda = 1$  and also for  $\epsilon' = \infty$  in the  $C_3$  geometry, the polarization of the system is made possible, during a MC run with a limited number of configurations, because in these cases the positive increase of the energy due to the polarization is small; in fact, it should be exactly zero if the system was approximately modeled by a dielectric continuum. When  $\lambda$  is smaller than 1 and  $\epsilon'$  is finite, these persistent polarized states disappear as a consequence of their unfavorable energies. This point is well illustrated (see Table I) by the comparison between the  $C_3$  data for  $\mu^{*2} = 2.75$ : at  $\epsilon' = \infty$ ,  $\bar{M}_{d,\alpha} \simeq 0.05 \pm 0.03$  and at  $\epsilon' = 0$ ,  $\bar{M}_{d,\alpha} \simeq 0.002 \pm 0.002$  and

by this between the  $S_3$  data for  $\mu^{*2} = 2$ : at  $\lambda = 0.8$ ,  $\bar{M}_{d,\alpha} \simeq 0.08 \pm 0.03$  and at  $\lambda = 0$ ,  $\bar{M}_{d,\alpha} \simeq 0.001 \pm 0.001$ . Table I shows also an influence of  $\epsilon'$  on the  $C_3$  data of  $U_{dd}$  and  $g_{dd}^{110}(\sigma)$ , which confirms that the value of  $N \sim 256$  is in this geometry the lower bound for getting reliable simulation results for dielectric fluids.

The conclusion of this discussion of  $S_3$  and  $C_3$  simulation data is that the  $S_3$  simulations of homogeneous dielectric fluids give, within the statistical uncertainty, identical results to the  $C_3$  simulations for  $\lambda = 0$  and  $N \gtrsim 256$  and for  $\lambda = 1$  and  $N \gtrsim 864$ .

### III. SIMULATIONS OF IONIC SOLUTIONS AND IONIC FLUIDS

The two ionic solutions studied in the  $S_3$  geometry are composed by 18 charged HS and 270 polar HS or by 54 charged HS and 810 polar HS, respectively. For this last system a computation<sup>7</sup> has been performed in  $C_3$  geometry for the numerical density  $\rho = 0.6$ , the ionic charge  $q^* (= q/\sigma kT) = 8$  and  $\mu^* = 1.775$ . It is worth noticing that for ionic system models there is no systematic study of possible size effects in  $C_3$  geometry. In Ref. 8 a comparison between simulation data of two systems of 10 ions and 246 solvent molecules and of 42 ions and 1024 solvent molecules seems to indicate that the size effects are rather small in  $C_3$  geometry for dense ionic solutions where  $q^* \sim 4$  and  $\mu^{*2} \sim 2$ . However, this comparison is certainly insufficient to conclude that within the range of the physically relevant values of  $q^*$ ,  $\mu^*$  and ionic or solvent densities, for systems of  $\sim 100$  ions and  $\sim 1000$  solvent molecules, the size effects will be small. However, we will make the hypothesis that the simulation data obtained in Ref. 7, which are also in good agreement with the results of the RHNC approximation, constitute a valid benchmark for testing the  $S_3$  simulation method.

The results of the  $S_3$  simulations are reported in Table II. Clearly, for the small system there are large discrepancies with the  $C_3$  results on the partial potential energies and the  $g^{000}(\psi)$  functions. For the other system ( $N = 864$ ), the agreement between the  $S_3$  and  $C_3$  data is rather satisfactory, but small differences remain for the partial energies.

The discrepancies at  $N = 288$  seem to be due to polarization effects. Specifically, the value of  $\langle \mathbf{M} \rangle$  is in average  $\sim 0$ , but the averages of the components of  $\mathbf{M}_i$  and  $\mathbf{M}_d$  have finite values (cf. the values of  $\bar{M}_{i,\alpha}$  and  $\bar{M}_{d,\alpha}$  in Table II). Similar to homogeneous dielectric fluids with  $\lambda \neq 0$  and  $N \sim 256$ , these metastable polarized states do not seem to relax towards an unpolarized state after  $10^7$  trial moves. For the system of 864 molecules, the polarization effects are weaker. The simulations in the  $S_3$  geometry are performed for  $\epsilon' = 0$  ( $\lambda = 0$ ), and in  $C_3$  geometry for  $\epsilon' = \infty$  ( $\lambda = 1$  in  $S_3$ ); these differences between the values of  $\epsilon'$  contribute to the discrepancies between the simulation data. An estimate of this contribution can be made by using the exact relation:

$$U(1) = U(0) - \frac{8\pi}{V} \mathbf{M}^2.$$

An approximated value of  $\langle U(1) \rangle_1$  is obtained from

$$\langle U(1) \rangle_1 \simeq \langle U(0) \rangle_0 - \frac{8\pi}{V} \langle \mathbf{M}^2 \rangle_0,$$

TABLE II. Simulations data for the ionic solutions.  $U$ ,  $U_{ii}$ ,  $U_{di}$ , and  $U_{dd}$  are the partial potential energies associated to  $U = \langle U(\lambda) \rangle$ .  $g_{++}^{000}$  (max) is the maximum value of the like-ion correlation functions, the other symbols are defined in the Table I caption and in the text (Sec. I). The partial energies at  $\lambda = 1$  are estimated by the procedure described in Sec. III.

$n \times 10^4$	$N_i$	$N_d$	$U_{ii}$	$U_{di}$	$U_{dd}$	$U$	$\bar{M}_{L,\alpha}$	$\bar{M}_{d,\alpha}$	$\frac{4\pi\beta}{3V} \langle M^2 \rangle$	$g_{++}^{000}$ (max)	$g_{+-}^{000}$ ( $\sigma$ )	$g_{dd}^{000}$ ( $\sigma$ )	$\lambda/\epsilon'$
31	18	270	-1.58 $\pm$ (3)	-2.68 $\pm$ (5)	-2.96 $\pm$ (2)	-7.232 $\pm$ (4)	-1.0 $\pm$ (2)	-0.06 $\pm$ (2)	0.97 $\pm$ (4)	-2.0 $\pm$ (3)	97 $\pm$ (4)	4.35 $\pm$ (1)	0 $S_3$
			-1.76 $\pm$ (3)	-2.38 $\pm$ (4)	-3.11 $\pm$ (2)	-7.238 $\pm$ (4)							1
26	54	810	-1.42 $\pm$ (2)	-2.98 $\pm$ (3)	-2.80 $\pm$ (2)	-7.206 $\pm$ (3)	-1.0 $\pm$ (2)	-0.07 $\pm$ (1)	0.99 $\pm$ (3)	1.1 $\pm$ (1)	67 $\pm$ (2)	4.276 $\pm$ (4)	0 $S_3$
			-1.47 $\pm$ (2)	-2.87 $\pm$ (3)	-2.85 $\pm$ (2)	-7.208 $\pm$ (3)							1
8	54	810	-1.51 $\pm$ (1)	-2.78 $\pm$ (3)	-2.88 $\pm$ (1)	-7.18			...	13 $\pm$ (1)	71 $\pm$ (2)	4.256 $\pm$ (4)	$\infty$ $C_3$

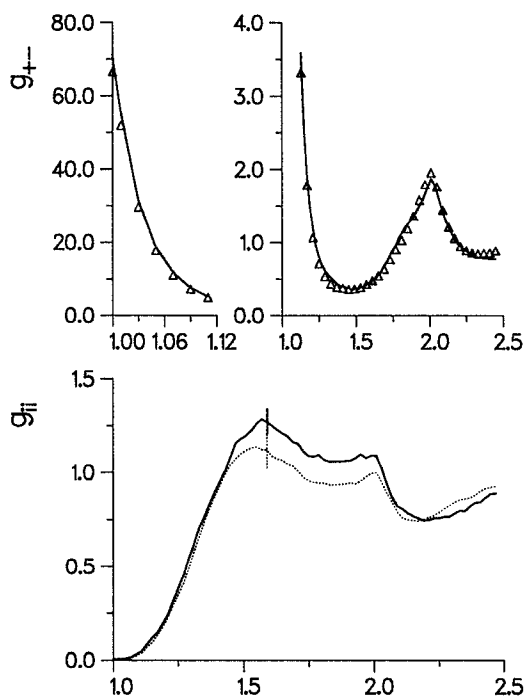


FIG. 2. From bottom to top, comparison between the like-ion correlation function  $g_{ii}$  and the unlike-ion correlation function  $g_{+-}$  for ionic solutions computed in  $C_3$  geometry (continuous line) at  $\epsilon' = \infty$  and in  $S_3$  geometry (dashed line or open triangles) at  $\lambda = 0$  with  $q^{*2} = 8$ ,  $N = 864$ , and  $\rho = 0.6$  ( $C_3$  results from Ref. 6). Typical error bars are given for the  $g_{ii}$  functions.

where  $\langle \dots \rangle_1$  and  $\langle \dots \rangle_0$  indicate ensemble averages computed for  $\lambda = 1$  and 0. This approximation is used to estimate the corrections on the partial energies:

$$\begin{aligned}
 \langle U(1) \rangle_1 &= \langle U_{ii}(1) \rangle_1 + \langle U_{di}(1) \rangle_1 + \langle U_{dd}(1) \rangle_1 \\
 &\simeq \langle U_{ii}(1) - (8\pi/V) \mathbf{M}_i^2 \rangle_0 \\
 &\quad + \langle U_{di}(1) - (16\pi/V) \mathbf{M}_d \cdot \mathbf{M}_i \rangle_0 \\
 &\quad + \langle U_{dd}(1) - (8\pi/V) \mathbf{M}_i^2 \rangle_0.
 \end{aligned}$$

The results of this correction procedure are given in Table II. For the large system the agreement between the data of the two geometries becomes excellent. For the smaller systems there is no improvement on the partial energies that clearly indicates that the differences with the  $C_3$  data are due to size effects. The polarization of the ionic and solvent components for  $N = 288$  does not preclude that the SL rule is satisfied because the polarization of the whole system is zero. The SL rule is also satisfied for the system  $N = 864$  with excellent accuracy.

In Figs. 2 and 3, we compare, respectively, the  $g_{ab}^{lmn}$  functions in the two geometries; the agreement shows that the expressions (12) give a reliable estimate of the correlations of the charged and dipolar HS in the solution. The differences between the two sets of functions for  $N = 864$  in  $C_3$  and  $S_3$  exceed the estimated statistical uncertainties, but they are not larger than a few percent. However, they indicate that, for  $N \sim 864$ , small size effects can affect, in  $S_3$ ,  $C_3$ , or both geometries, the values of the correlation functions

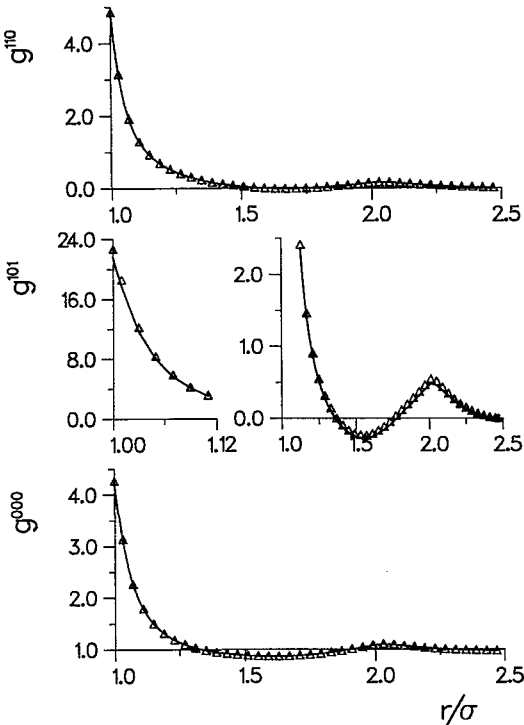


FIG. 3. Same as in Fig. 3. Comparison between the  $g^{lmn}$  functions of ionic solutions for solvent-solvent correlation functions ( $g_{dd}^{000}$  and  $g_{dd}^{110}$ ) and ion-solvent correlation function  $g_{id}^{101}$ .

which depend weakly on the choice of  $\epsilon'$  and  $\lambda$ . The simulation data reported in Table III concern a mixture of charge HS which is the generic model of the restrictive primitive models of electrolyte. They show the influence of a nonzero value of  $\lambda$  on the thermodynamic properties and the correlation functions of an ionic system. The comparison with the data obtained in Ref. 1 and the SL rule can be used to estimate the importance of the size effects introduced by using  $\lambda \neq 0$ . For  $\lambda = 0.5$ , the formulas (9) of the SL rule give  $4\pi\beta \langle \mathbf{M}_i^2 \rangle / 3V = 4$ . Within the statistical error, this value is only obtained for a system size of  $N = 256$ . In this case, the energy and the correlation functions (cf. Fig. 4) are identical with the result obtained for  $\lambda = 0$  and  $N = 256$ . For the small sizes  $N < 128$  with  $\lambda = 0.5$  and also for  $\lambda = 1$ , the ionic fluids acquire a strong polarization due to the interaction potential term depending on  $\lambda$  which generates an attractive pair potential between the ions

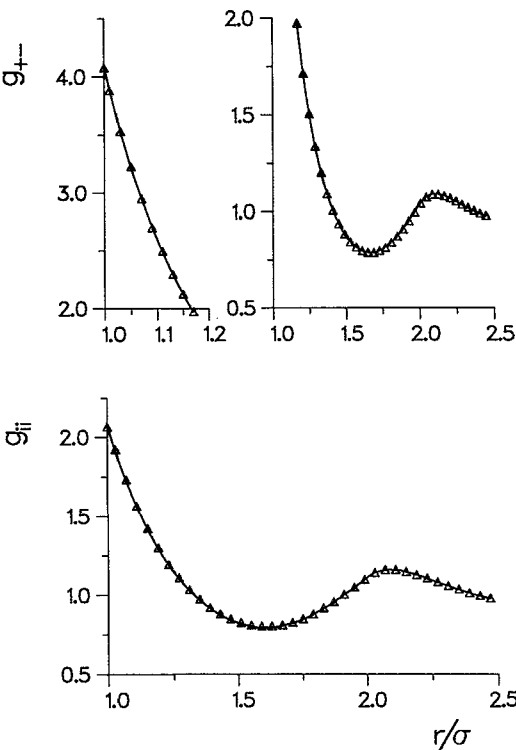


FIG. 4. From bottom to top, comparison between the correlation functions for homogeneous ionic fluids computed in  $S_3$  geometry at  $\lambda = 0$  (continuous line) and  $\lambda = 0.5$  (open triangles) for  $\rho = 0.674$ ,  $q^2(4\pi p/3)^{1/3}/kT = 2$ , and  $N = 256$ .

of the same charge. For small systems, this attractive potential becomes of the same order as the charge-charge interaction. For  $\lambda = 1$ , we do not attempt to evaluate the values of  $N$  such as the induced polarization gives only a small bias ( $\sim 1\%$ – $2\%$ ) on the thermodynamic properties. It is worth noticing that, in the  $C_3$  geometry, the term  $2\pi\mathbf{M}_i^2/V(2\epsilon' + 1)$ , introduced in the Ewald energy to account for the influence of an external dielectric continuum, generates also a similar attractive potential between the like ions. But, the induced polarization is, for an equal value of  $N$ , weaker than in  $S_3$  geometry. Finally, these new simulations of homogeneous ionic fluids at  $\lambda \neq 0$  confirm the conclusion obtained in Ref. 1, that reliable data can be obtained in  $S_3$  geometry when the system size is larger than  $N = 256$ . This conclusion stays valid for all values of  $\lambda < 0.5$ .

TABLE III. Simulation data for ionic fluids in  $S_3$  geometry at  $\lambda \neq 0$  and  $q^2(4\pi p/3)^{1/3}/kT = 2$ . The last column gives the variation of the numerical density if the packing fraction is kept constant (Ref. 1). The symbols are defined in the text and in Tables I and II. The results at  $\lambda = 0$  are from Ref. 1.

$N$	$n \times 10^4$	$U_{ii}$	$\bar{M}_{i,\alpha}$	$g_{++}^{000}(\sigma)$	$g_{+-}^{000}(\sigma)$	$\frac{4\pi\beta}{3V} \langle \mathbf{M}_i^2 \rangle$	$\lambda$	$N\sigma^3/V$
32	10	$-0.765 \pm (1)$	$\sim 0.02 \pm (2)$	$2.22 \pm (2)$	$3.93 \pm (3)$	$6.6 \pm (3)$	0.5	0.688
64	20	$-0.731 \pm (1)$	$\sim 0.01 \pm (1)$	$2.10 \pm (1)$	$4.06 \pm (1)$	$6.0 \pm (3)$	0.5	0.680
128	15	$-0.727 \pm (1)$	$\sim 0.01 \pm (1)$	$2.12 \pm (1)$	$4.15 \pm (1)$	$5.1 \pm (3)$	0.5	0.678
256	9	$-0.728 \pm (1)$	$\sim 0.005 \pm (5)$	$2.06 \pm (1)$	$4.07 \pm (1)$	$4.4 \pm (3)$	0.5	0.674
256	4	$-0.728 \pm (3)$	...	$2.08 \pm (3)$	$4.11 \pm (3)$	$1.03 \pm (3)$	0	0.674

## CONCLUSIONS

In this study we have established the validity of the  $S_3$  method for the numerical simulations of the dielectric fluids and the ionic solutions. As for the ionic fluids,<sup>1</sup> this method is for these systems an efficient alternative to the Ewald method. Our simulations have allowed us to verify the complete analogy between the  $C_3$  and  $S_3$  geometries established theoretically in Ref. 4. Both  $C_3$  and  $S_3$  methods have shortcomings. In  $S_3$ , the most important defect is the use of non-Euclidean confining volumes, which can preclude the simulations of solid phases. For the  $C_3$  geometry, the defect is the cubic symmetry of the interaction potential which implies a similar symmetry of the correlation functions. In both geometries the consideration of a potential energy accounting for the influence of a dielectric continuum external to the simulated system can induced metastable polarizations. The size effects resulting from these deficiencies are most important for the low values of  $N$  ( $\sim 100$ ) in the  $S_3$  geometry. This has the consequence that reliable simulations of dielectric fluids must be performed for a system size of  $N > 200$ , and those of ionic solutions for an ionic concentration of  $\sim 1$  mol with  $N_i \sim 100$  and  $N_d \sim 1000$ . In spite of these limitations, the  $S_3$  method has a numerical efficiency better than the  $C_3$  method. This point is made clear by the account of the number of floating operations needed for the calculation of the potential energy of one charged HS of an ionic mixture in the two geometries. This number is equal to  $\sim 9N$  in  $S_3$  and  $\sim 20n_c + 40n_k$  in  $C_3$ , where  $n_c$  is the number of considered

neighboring molecules in the calculation of the  $r$ -space term of the Ewald energy and  $n_k$  is the number of  $k$  vectors used for the computations of the  $k$ -space term. This estimate of the floating operations supposes that, obviously, convenient tables of the elements of the pair potential depending only on  $\psi(S_3)$  and  $r$  or  $k(C_3)$  have been made.

In most of the simulations, for an accurate estimate of the Ewald energy,  $n_c$  and  $n_k$  must be taken on the order of 300 and 200; with these figures, the  $S_3$  simulations are certainly more efficient than the  $C_3$  simulations for  $N \leq 1500$ –2000. The reliability of the  $S_3$  method allows us to realize simulations of inhomogeneous dielectric fluids and ionic solutions near a charged interface, physical systems which should be two of its main applications. Indeed, the Ewald method needs a large amount of computer times if it is used for the simulation of inhomogeneous systems, due to the breaking of the periodicity of the boundary conditions in one of the space's directions.<sup>9</sup>

<sup>1</sup> J. M. Caillol and D. Levesque, J. Chem. Phys. **94**, 597 (1991).

<sup>2</sup> S. W. de Leeuw, J. W. Perram, and E. R. Smith, Proc. R. Soc. London, Ser. A **373**, 27 (1980).

<sup>3</sup> B. Cichocki, B. U. Felderhof, and K. Hinsen, Phys. Rev. A **39**, 5350 (1989).

<sup>4</sup> J. M. Caillol, J. Chem. Phys. **96**, 1455 (1992).

<sup>5</sup> J. Tobochnik and R. M. Chapin, J. Chem. Phys. **88**, 5824 (1988).

<sup>6</sup> P. G. Kusalik, J. Chem. Phys. **93**, 3520 (1990).

<sup>7</sup> J. M. Caillol, D. Levesque, and J. J. Weis, Mol. Phys. **69**, 199 (1990).

<sup>8</sup> J. M. Caillol, D. Levesque, and J. J. Weis, J. Chem. Phys. **91**, 555 (1989).

<sup>9</sup> D. M. Heyes, M. Barber, and J. M. R. Clarke, J. Chem. Soc. Faraday Trans. 2 **73**, 1485 (1977).